The possible importance of synchrotron/inverse Compton losses to explain fast MM-wave and hard X-ray emission of a solar event

ARTICLE · MARCH 1986

Source: NTRS

5 AUTHORS, INCLUDING:

Emilia Correia

National Institute for Space Research, Brazil

105 PUBLICATIONS **527** CITATIONS

SEE PROFILE

J. E. R. Costa

National Institute for Space Research, Brazil

115 PUBLICATIONS **605** CITATIONS

SEE PROFILE

Brian R Dennis

NASA

426 PUBLICATIONS **6,550** CITATIONS

SEE PROFILE

THE POSSIBLE IMPORTANCE OF SYNCHROTRON/INVERSE COMPTON LOSSES TO EXPLAIN FAST MM-WAVE AND HARD X-RAY EMISSION OF A SOLAR EVENT

E. Correia, P. Kaufmann, J. E. R. Costa, and A. M. Zodi Vaz

INPE: Instituto de Pesquisas Espaciais
C.P. 515, 12.200-São José dos Campos, S.P., Brazil

B. R. Dennis

Laboratory for Astronomy and Solar Physics
NASA: Goddard Space Flight Center
Greenbelt, MD 20771

ABSTRACT

The solar burst of 21 May 1984 presented a number of unique features. The time profile consisted in seven major structures (seconds), with a turnover frequency $\tilde{>}$ 90 GHz, well correlated in time to hard X-ray emission. Each structure consisted in multiple fast pulses (10^{-2} seconds), which were analysed in detail. It has been confirmed a proportionality between the repetition rate of the pulses and the burst fluxes at 90 GHz and $\tilde{>}$ 100 keV hard X-rays, and found an inverse proportionality between repetition rates and hard X-rays power law indices. A synchrotron/inverse Compton model has been applied to explain the emission of the fast burst structures, which appear to be possible for the first three or four structures.

A number of unique characteristics were found in a solar event observed in 21 May 1984, 1326UT at 30 and 90 GHz by Itapetinga Radio Observatory using high time resolution (1 ms) and high sensitivity (0.03 S.F.U.), and at hard X-rays by the HXRBS experiment on board of the SMM satellite, with 128ms time resolution. This event was also observed by patrol radio telescopes at 7 GHz (Itapetinga) and at 1.4, 2.7, 5, 8.8 and 15.4 GHz (AFGL; Cliver, 1984). The time profiles at hard X-rays, in two energy ranges, and at 90, 30 and 7 GHz radio frequencies are shown in Figure 1.

The event presented seven major time structures (1-2 sec duration) at 90 GHz, very well correlated to hard X-rays. They are labeled A-G in Figure 1. The 30 GHz emission enhanced only after the fourth structure, and was also well correlated to the 90 GHz and hard X-rays emissions. The radio emission intensity increased towards the shortest mm-waves, indicating a turnover frequency at about or above 90 GHz for all seven major time structures, as shown by the spectra in Figure 2.

Table I - Parameters of the burst major time structures, labeled A-G(Figure 1). The spectral indices α and q are mean values at the maximum of each structure. Radio fluxes are in s.f.u., 1 s.f.u. = 10^{-22} w/m^2 Hz, and X-ray fluxes are in units of 3 x 10^{-25} erg/cm^2 s Hz. R is the repetition rate of fast pulses for each structure, R = N/Δt, with N the number of pulses, and Δt the duration of the major structures (or packet of pulses).

Structure	Flux 90 GHz	Flux 30 GHz	Flux X-ray >30 keV	Flux X-ray >100 keV	spectral indices burst $\bar{\alpha}$	spectral indices burst $\bar{q}$	spectral indices slow comp. $\bar{\alpha}$	spectral indices slow comp. $\bar{q}$	packet dur. (sec)	Nº pulses N	R (s^{-1})	e-fold. rise time(ms)	ΔF/F 90 GHz
A	8	3	0.2	0.01	1.2	2.2	0.8	4.0	2.0	3	1.5	60	50
B	34	5	0.6	0.03	1.8	2.5	0.8	4.0	3.8	11	2.9	70	20
C	83	7	0.7	0.05	2.5	1.9	1.0	3.0	2.8	14	5.0	40	50
D	40	9	0.4	0.02	1.6	2.7	4.0	3.4	1.6	5	3.0	60	20
E	58	24	1.1	0.04	0.9	2.4	0.3	3.4	1.7	6	3.5	50	30
F	27	12	0.6	0.02	0.7	2.8	0.3	3.4	1.6	4	2.5	60	50
G	23	16	0.5	0.03	0.3	2.7	0.0	3.5	1.0	3	3.0	60	40

Interesting properties are found by correlating pulse repetition rates and the fluxes at 90 GHz and X-rays, for the various packets of pulses. The scatter diagrams (Figure 6) are for the seven structures which, together, included 46 fast pulses. The correlation coefficient was excellent at $\gtrsim$ 100 keV X-rays and 90 GHz (better than 90%) but not so good at $\gtrsim$ 30 KeV X-rays (60%). These results favour the well accepted assumption that the mm-wave emission are better associated to the higher energy X-rays and confirm the idea that the pulses emission are quasi-quantized in energy (Kaufmann et al., 1980; Correia, 1983; and Loran et al., 1985). The characteristic energy radiated by each pulse at the emitting source can be estimated as 5 x 10^{20} ergs at 90 GHz and 10^{20} ergs at $\gtrsim$ 100 KeV X-rays.

Another and new result was found by correlating the pulse repetition rates and hard X-ray power-law spectral index, shown in Figure 7. The correlation coefficient is very good (91%). This result suggest that the harder is the spectrum, the larger is the repetition rate.

The fast pulse emission and the high radio turnover frequency are difficult to be interpreted using models currently available which consider the acceleration of non-relativistic or mildly relativistic electrons (Kaufmann et al., 1985; and McClements and Brown, 1986).

One possible explanation assumes the acceleration of ultrarelativistic electrons which produce a synchrotron emission component spectrum peaking somewhere at $\nu \gtrsim 10^{11}$ Hz. The concurrent hard X-ray emission is attributed to inverse Compton quenching on the synchrotron photons produced in a compact, bright and short-lived source (Kaufmann et al., 1986). We analysed here this possible interpretation for all the seven major structures of the 21 May 1984 event.

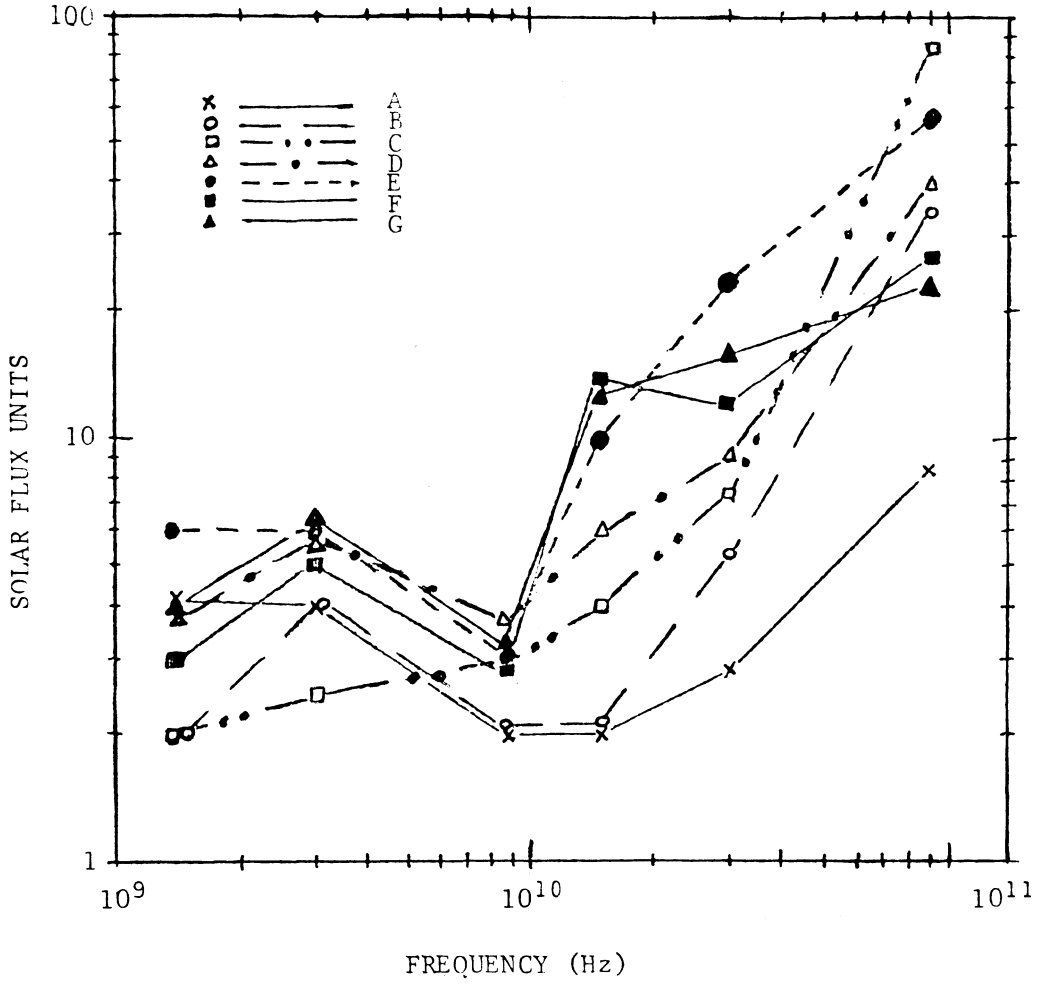

Figure 2 - Radio spectra for the maximum of each major time structure of the 21 May 1984 event, as indicated in Figure 1.

Table I summarizes the main characteristics of each major time structure of the burst. The spectral indices of the burst structures are distinguished from the indices of a slow underlying burst emission component (~20 seconds). At radio, the spectral indices α are defined as $F \propto \nu^{\alpha}$, where F is the flux density and ν the frequency. The spectral indices between 30-90 GHz enhanced for each superimposed structure with $\alpha \sim 0.3 - 2.5$, while the underlying slow component spectral index was varying slowly in the 0-1.0 range. The X-ray power-law spectral indices δ are defined as $F \propto E^{-q}$, where F is the flux, E the photon energy, and $q = \delta - 1$. The corresponding hard X-ray structures exhibited spectral indices reduction to ≈ 3, while the slow component remained at the $\delta \sim 4-5$. The spectra become harder in peak of each structure (Figure 5, Table I).

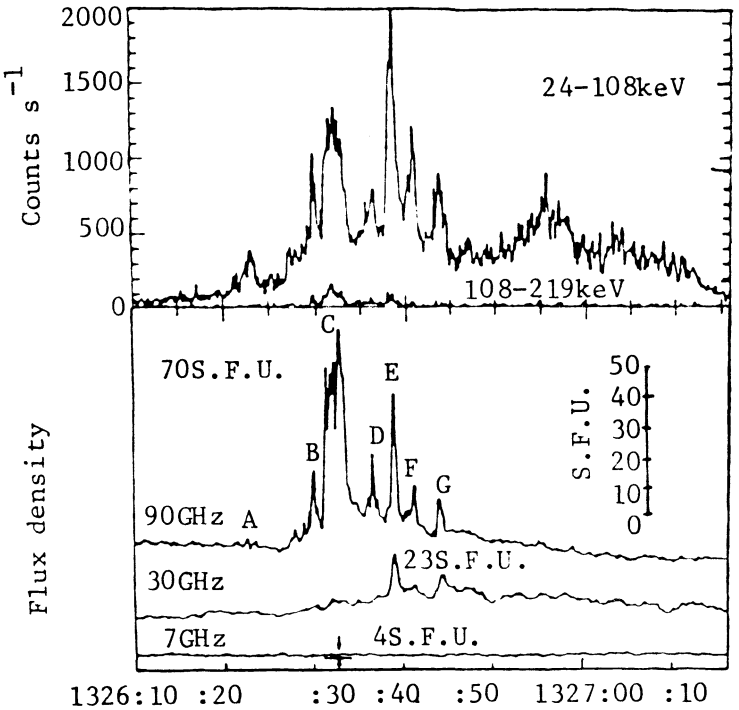

Figure 1 - The solar burst of 21 May 1984, 1326UT, observed at 7, 30 and 90 GHz (Itapetinga Radio Observatory) and hard X-rays (HXRBS-SMM). The seven major time structures are labeled A-G.

Each structure was expanded in 4 second sections, in order to analyse their time profiles in more detail. Using running mean technique,we filtered the 4 seconds sections to evidence pulses at 30 and 90 GHz (Figure 3). The plots show that each radio structure, consisted in packets of fast pulses with durations of tens of milliseconds and relative amplitude of ~50% at 90GHz and of less than 5% at 30GHz. After the fourth structure, when the 30 GHz emission was enhanced, we verified that the pulses between 30 and 90 GHz were generally in phase, to better than 10 ms (Figure 4).

Time expanded 4s sections were also analysed in comparison to hard X-rays, and in terms of spectral indices. Two examples are shown in Figure 5. At X-rays, the pulses are not visible because their durations (~60 ms) are shorter than the time resolution available (~128 ms). However, when compared with time integrated 90 GHz data, in the same 128 ms, the overall time structures appear to be well correlated. Therefore it is likely that the fast pulses are also present at hard X-rays and would be detected if enough sensitivity, and time resolution were available. In this case, it is plausible to assume that both, the radio and hard X-ray pulses, are produced by the same population of energetic electrons.

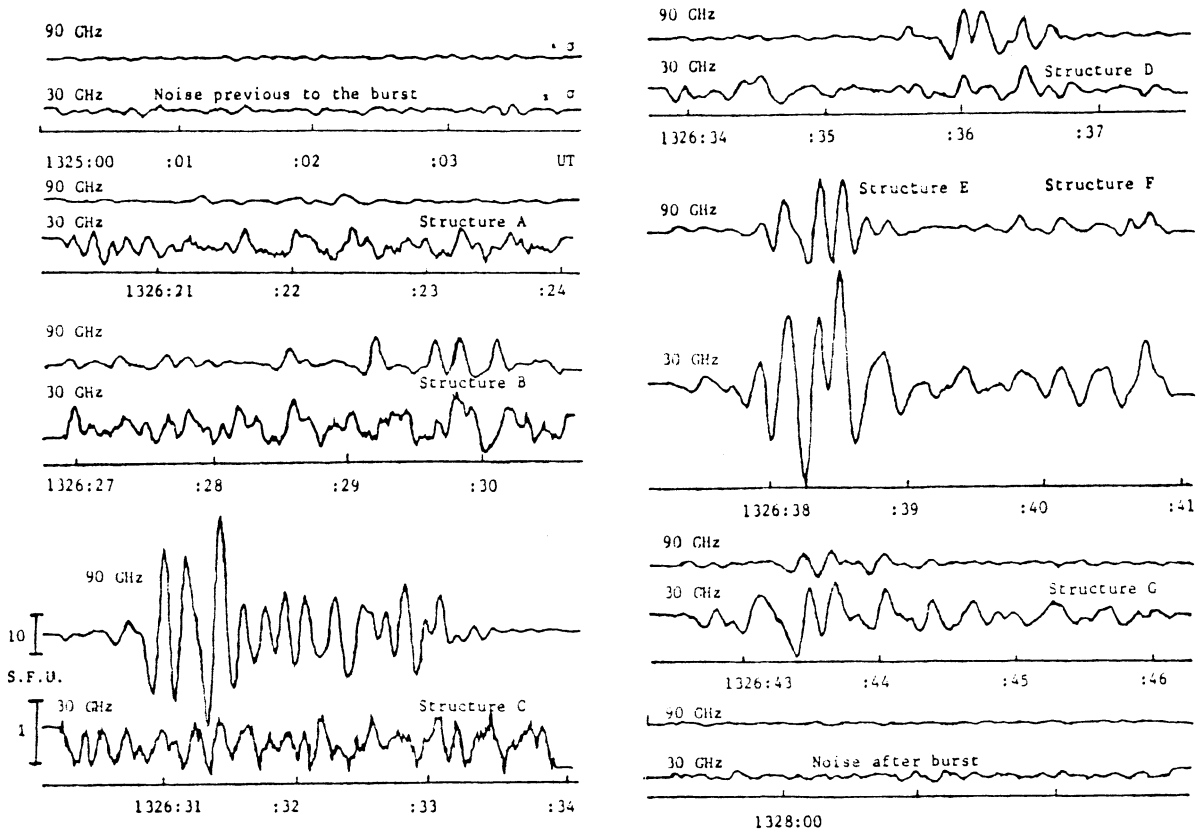

Figure 3 - All the structures at 90 and 30 GHz plotted on a 4s expanded time scale with a running mean subtracted from the measured fluxes at the two frequencies. The flux scales are indicated for structure C, and are kept the same for all the other 4s sections.

Using the formulation of the synchrotron/inverse Compton model given by Kaufmann et al., (1986), we obtained the pulse source characteristics in each one of major time structures. The results, considering a magnetic field of 500 gauss are given in Table II.

The application of the synchrotron/inverse Compton model seems to work self-consistently in the first four major time structures(A, B, C, D), which have turnover frequencies well above 10^{11} Hz. The estimated source parameters required to explain the high turnover frequency and the short pulse durations (~ 60 ms) are: source of $\sim 10^{7}$cm and $\sim 10^{11}$ cm^{-3} density of energetic electrons with Lorentz factor $\gamma \gtrsim 40$. The model predicts a turnover frequency around 10^{13} Hz.

For the last three structures (E, F, and G) exhibiting a turnover frequency at about 10^{11} Hz, the application of the model would require unrealistically high numbers of energetic electrons. The last three structures might be explained by existing models that do not require the acceleration of ultrarelativistic electrons (for example: Dulk and Marsh, 1982).

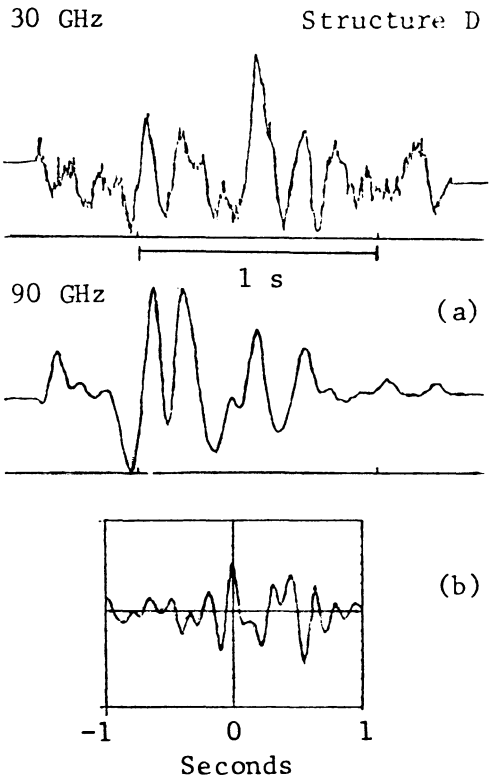

Figure 4 - Phase relationships are analysed for Structure D, with the pulses time profile in (a), and their cross-correlation in (b). Pulses are in phase to an accuracy better than 10ms.

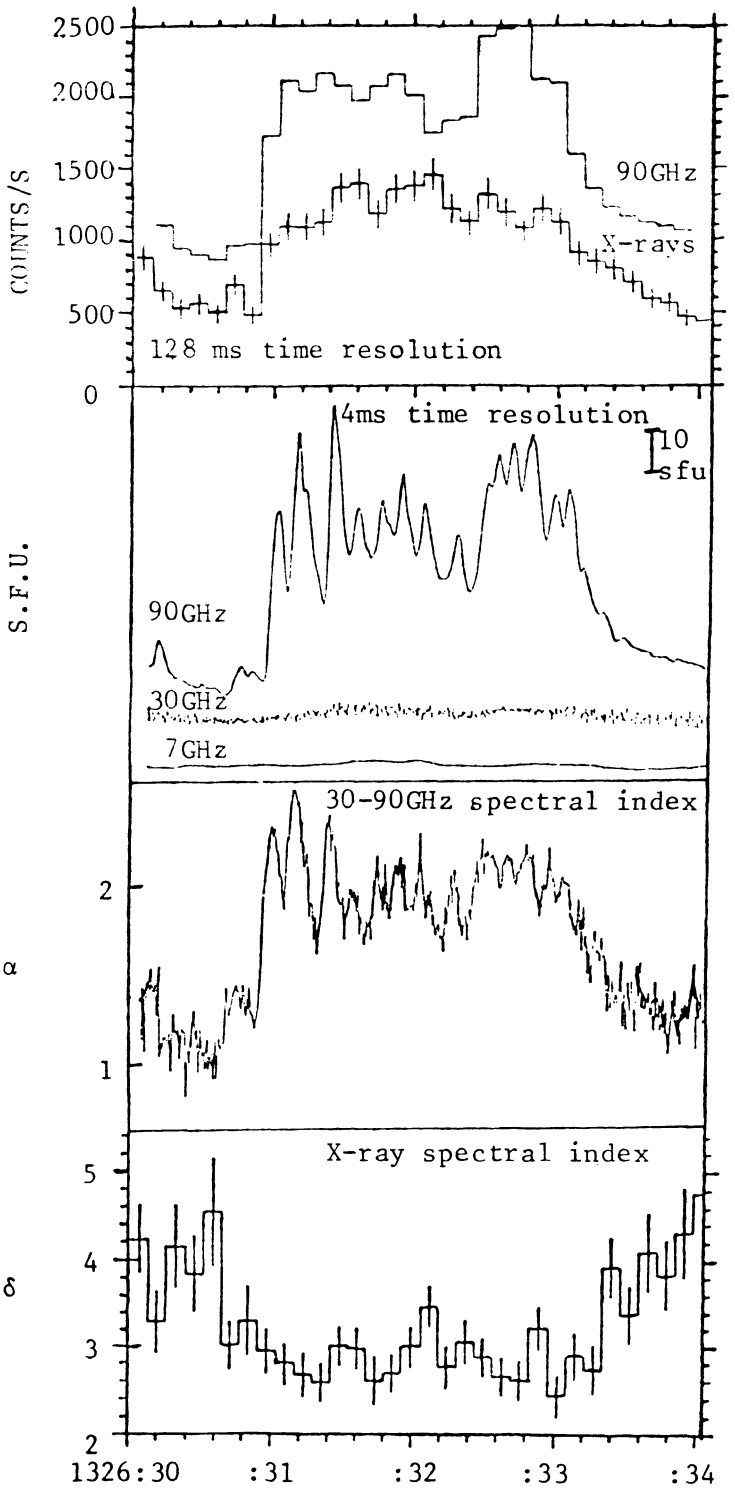

Figure 5(a) - A comparison of flux and spectral indices at 90 and 30 GHz, and hard X-rays (> 30 keV) for Structure C. The time resolution at hard X-rays was 128 ms, and at radio was 4 ms. In the upper plot the 90 GHz data was time integrated in 128 ms, in order to compare to the X-rays time profile.

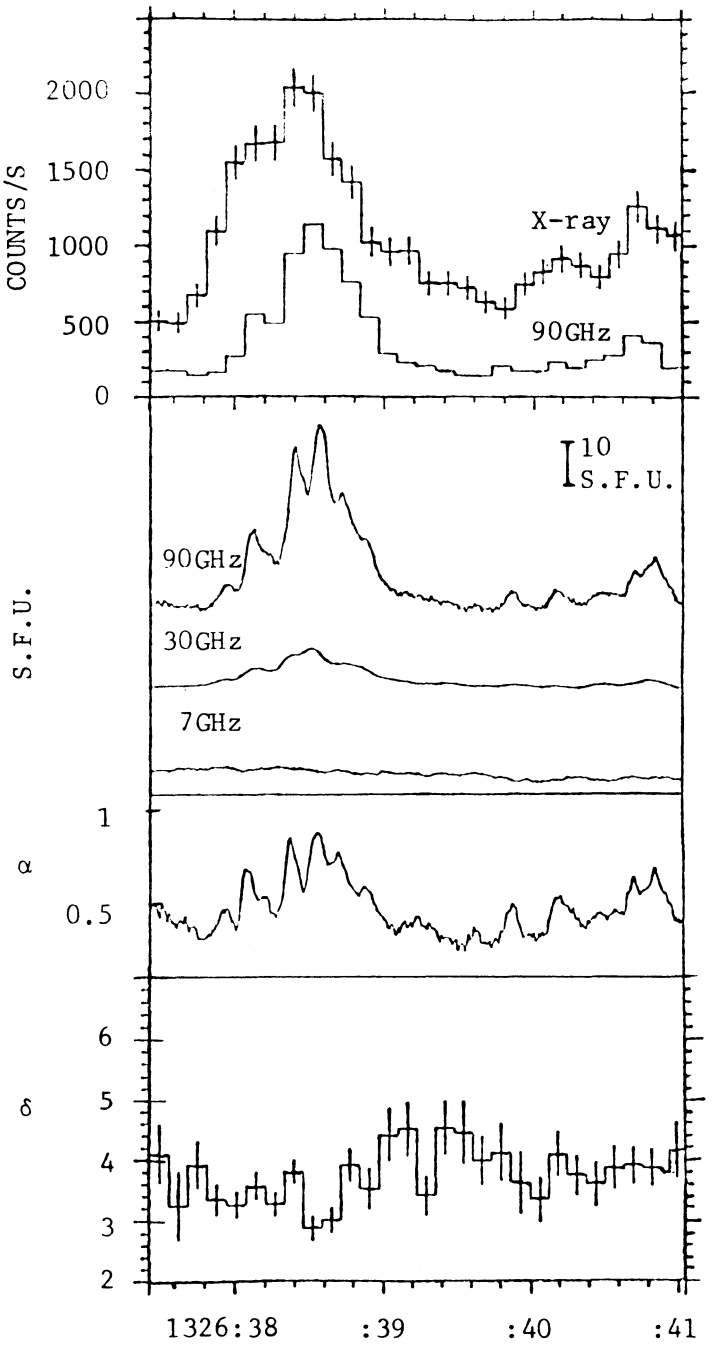

Figure 5(b) - Comparative plots, similar to Figure 5(a), for Structure E.

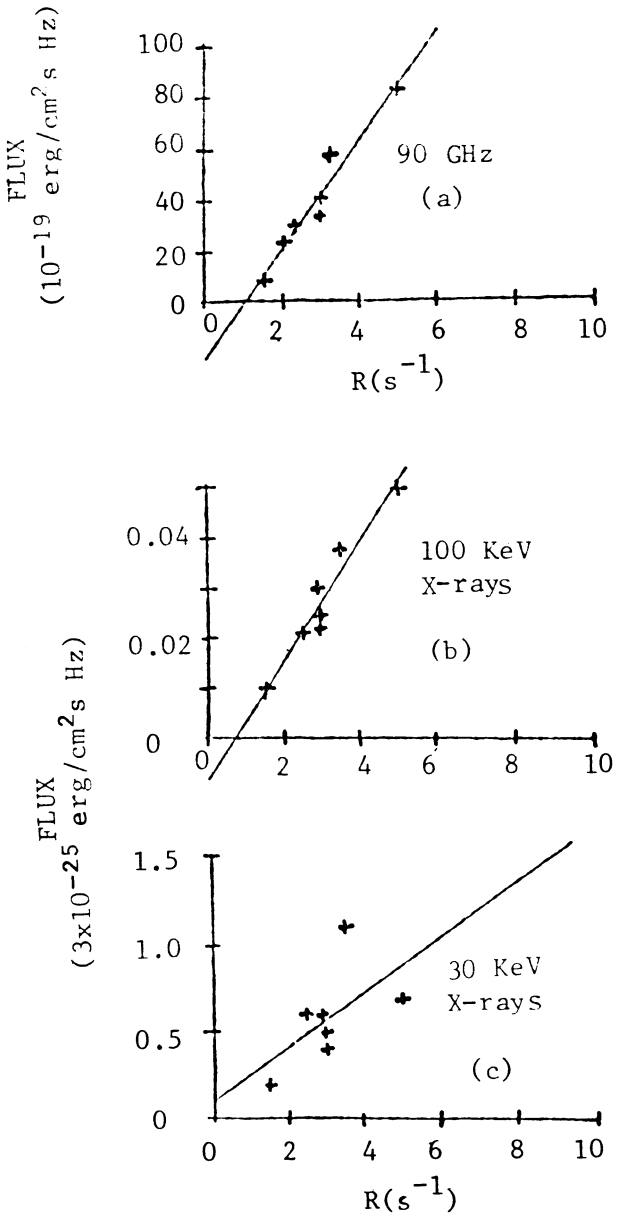

Figure 6 - Scatter diagrams: (a) Pulse repetition rates and fluxes at 90 GHz, (b) repetition rates at 90 GHz and fluxes at hard X-rays (> 100 keV), and (c) repetition rates at 90 GHz and fluxes at hard X-rays (> 30 keV), for all the seven structures.

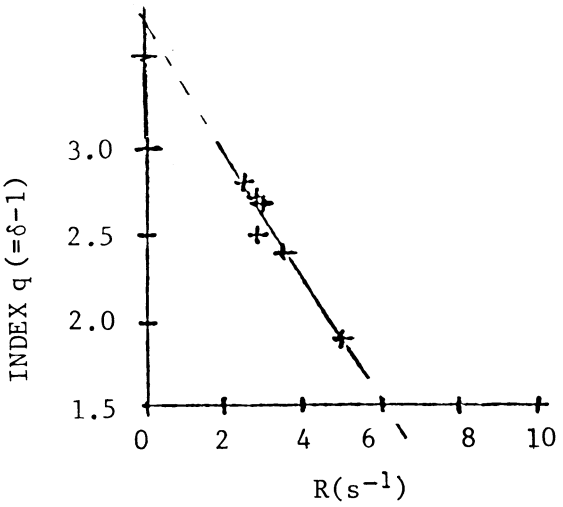

Figure 7 - Scatter diagram between pulse repetition rates and X-ray spectral index, for the last six burst structures.

Table II - Pulse source characteristics defined by Kaufmann et al., (1986) synchrotron/inverse-Compton model application of each major time structure as labeled in Figure 1. Parameters are defined at times $t = t_o$ (at the begining of the pulse) and $t = t_p$ (at the maximum of the pulse radio emission). γ is the Lorentz factor, ξ is the fraction of energy lost by the electrons, $\xi = \gamma(t = t_p)/\gamma(t = t_o)$; ν_{sm} is the maximum frequency of the spectrum produced by the accelerated ultrarelativistic electrons; K is the proportionality factor of the power law distribution $N(\gamma) = K\gamma^{-n}$; N and N_t are the density and total number of electrons accelerated per pulse; $r_{c/B}$ is the ratio of the inverse-Compton to bremsstrahlung losses "intrinsic" to the emitting pulse source.

STRUCTURE	ν_{sm} $(t=t_o)$ Hz	ν_{sm} $(t=t_p)$ Hz	ξ	KV electrons	N_t electrons	N cm^{-3}	γ $(t=t_p)$	$r_{c/B}$ t_o	$r_{c/B}$ t_p	scale size cm
A	7×10^{13}	3×10^{12}	0.21	2×10^{39}	2×10^{31}	2×10^{10}	47	10^7	10	10^7
B	8×10^{13}	4×10^{12}	0.26	10^{41}	2×10^{32}	2×10^{11}	40	10^7	56	10^7
C	7×10^{13}	2×10^{12}	0.17	4×10^{38}	8×10^{31}	8×10^{10}	39	10^7	2	10^7
D	9×10^{13}	4×10^{12}	0.21	9×10^{41}	2×10^{32}	2×10^{11}	45	3×10^7	24	10^7

Acknowledgements

This research was partially supported by the Brazilian research agency FINEP. INPE operates CRAAM and Itapetinga Radio Observatory. One of the authors (PK) is Guest Investigator on NASA-SMM Project.

REFERENCES

Cliver,E.W.: 1984, *private communication.*

Correia,E.: 1983, MS thesis, INPE, Brazil.

Dulk,G.A.; and Marsh,K.A.: 1982, *Astrophys.J.*, **259**, 350.

Kaufmann,P.; Strauss,F.M.; Opher,R.; Laporte,C.: 1980, *Astron. Astrophys.*, **87**, 58.

Kaufmann,P.; Correia,E.; Costa,J.E.R.; Zodi Vaz,A.M.; and Dennis,B.R.; 1985, *Nature*, **313**, 380.

Kaufmann,P.; Correia,E.; Costa,J.E.R.; and Zodi Vaz,A.M.: 1986, *Astron. Astrophys.*, in press.

Loran,J.M.; Brown,J.C.; Correia,E.; and Kaufmann,P.: 1985, *Solar Phys.*, **97**, 363.

McClements,K.G.; and Brown,J.C.: 1986, *Astron. Astrophys.*, submitted.